Proceedings of the 25th International Conference on
Port and Ocean Engineering under Arctic Conditions
June 9-13, 2019, Delft, The Netherlands

Ice loads on an axi-symmetric vessel due to managed first-year ridges

Ken Croasdale[1]
[1] K R Croasdale & Associates Ltd., Calgary, Canada

ABSTRACT

Depending on water depths and ice conditions, floating systems are often the preferred approach to drilling and production in ice-covered waters. An axi-symmetric vessel has the advantage of presenting the same profile to the ice regardless of ice direction. In most ice areas of interest, it is envisaged that such vessels would be operated with ice management to keep the mooring forces within acceptable levels.

In many areas, the first-year ridge can be the most critical ice feature for loads on platforms. However, ice ridges can be difficult to break up into small pieces and methods to reduce the amount of ice management whilst still leading to acceptable mooring loads are desired.

The primary ice management hypothesis investigated in this study is that of isolating a ridge from the surrounding ice sheet such that it fails by in-plane bending at low ice loads.

A new model for the in-plane bending failure of a ridge was developed based on composite beam theory. Out-of-plane failure of a ridge on a downward slope was also analysed using bounding techniques in order to assess initial penetration of the ridge which then reduces the failure load for in-plane bending. This mode of failure also applies to short ridges.

The theoretical models were compared to experimental data from model tests which are in the open literature.

KEY WORDS Vessels; Ice-management; Ridges; Mooring loads

NOMENCLATURE

b – ridge width
c - cohesion of keel rubble
D – contact width between ridge at platform
F – force (ridge failure force and load on platform)
h - thickness
h_r – ridge thickness
h_k – keel thickness
$h_{k\ effective}$ – equivalent rectangular shaped keel
h_{ki} – equivalent solid ice thickness of keel for in-plane bending
h_{cl} – thickness of consolidated layer of ridge
I – second moment of area
L – ridge length

M – bending moment
s – distributed load acting between ridge and platform
w– distributed load on back of ridge
y – distance from neutral axis to edge of ridge
σ_f – flexural strength of ice
σ_{keel} – effective strength of keel (flexure)
σ_{cl} – flexural strength of consolidated

DEFINING THE PROBLEM

The problem addressed is that of an axi-symmetric floating moored vessel subject to the action of first-year ridges. It is assumed that to lower the mooring loads the oncoming ice is "managed". It is further assumed in framing the problem that the primary ice management objective is to reduce the ice loads from first-year ridges. As in all ice management activities the goal would be to do the minimum ice breaking to achieve the mooring load reduction.

Ridges themselves can be formidable ice features to break into smaller pieces. Studies have shown that ridge keels can have thicknesses about 15 – 20 times the level ice thickness and consolidated layers 1.5 – 3 times as thick as level ice. A ridge is similar to a mountain range; in plan view it is often sinuous, see Figure 1, but for engineering purposes ridges are approximated to linear features.

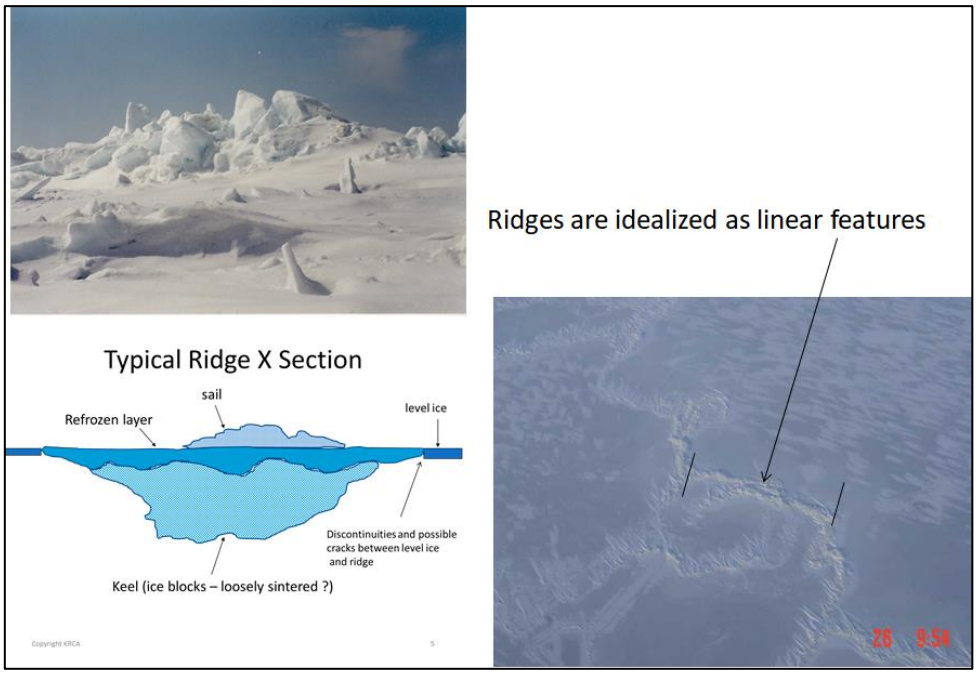

Figure 1: Morphology of a pressure ridge

To break a ridge across its width can require significant forces and ice management effort. So one potentially easier tactic may be to isolate the ridge from its surrounding ice sheet and encourage the ridge to fail by in-plane bending as it advances on a moored platform. This is shown conceptually in Figure 2.

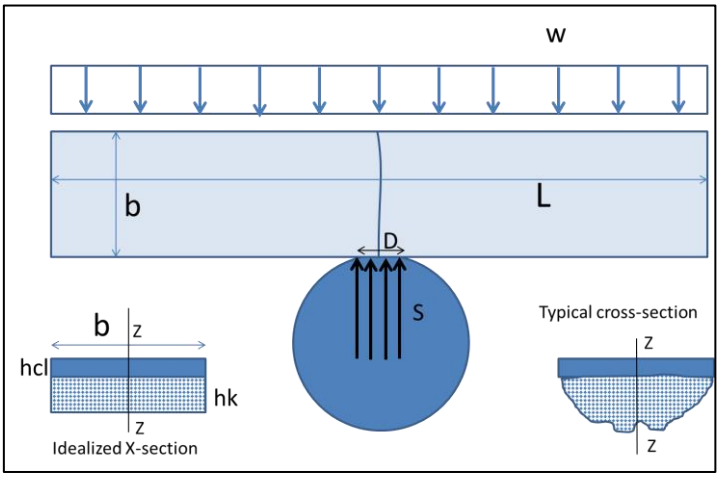

Figure 2: In-plane bending of a ridge

IN-PLANE BENDING

Load to fail

Referring to Figure 2, the bending moment at the centre of the beam is given by

$$M = wL^2/8 - sD^2/8 \quad (1)$$

For balance of forces,

$$s = wL/D \quad (2)$$

Therefore,

$$M = wL(L-D)/8 \quad (3)$$

The next step is to relate M to the in-plane bending capacity of the ridge. If the ridge was made of a homogeneous material, the engineer's theory of bending applies,

$$M = \sigma_f I/y \quad (4)$$

For a solid rectangle with width b and thickness h,

$$I/y = b^2h/6 \quad (5)$$

Combining (3), (4) and (5), the value of w to create a centre crack failure is given by,

$$w = 1.33b^2h\sigma_f/(L(L-D)) \quad (6)$$

The load at failure (F) is then,

$$F = wL = 1.33b^2h\sigma_f/(L-D) \quad (7)$$

Equivalent cross section

First-year pressure ridge keels are often of trapezoidal or triangular shape as depicted in Figure 3. The first step in developing an equivalent cross section is to idealize the keel into a rectangle to give the same I value about the Z-Z axis. If the keel was a triangle it can be shown that $h_{keffective} = 0.25h_k$. Most ridges will be trapezoids with varying bottom width which would increase the 0.25 value in the relationship. In this work we will use a value of 0.5 (the results are not very sensitive to this value).

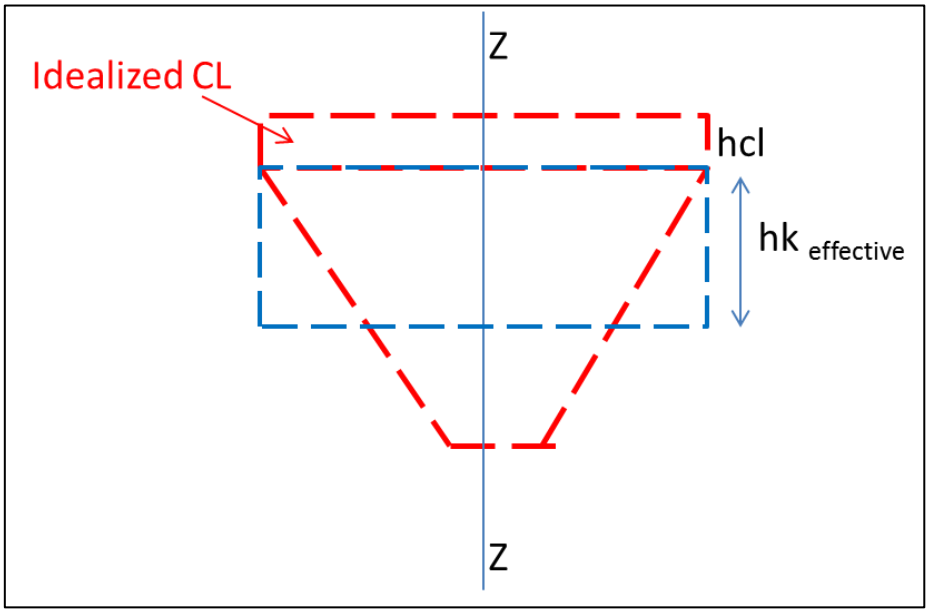

Figure 3: Effective rectangular keel creating a composite beam (for same Iz-z)

The next step is to convert the composite beam of solid ice rectangle and a rubble rectangle into an equivalent solid beam for bending about the z-z- axis (Figure 4)

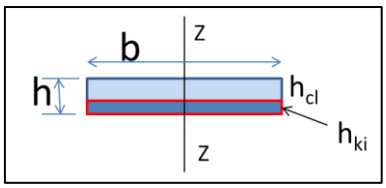

Figure 4: Solid ice beam equivalent to the composite beam

$$h = h_{cl} + h_{ki} \quad (8)$$

For bending about the Z-Z axis, shear compatibility is not needed between the two materials, so the equivalent thickness of the keel as solid ice is simply based on flexural strengths. Hence,

$$h = h_{cl} + (\sigma_{keel}/\sigma_{cl}/)h_{k\ effective} \quad (9)$$

These strength values are "flexural" or tensile. Little is known about the tensile strength of ice rubble, but some work has been done at field scale; (reported in Croasdale, 2012). For full scale keel rubble, a typical high value is about 25kPa. (Note where c values (cohesion) for the keel are reported, it is assumed that $\sigma_{keel} = 2c$).

Example

The prior theory is now applied to a typical extreme first-year ridge. Assume the ridge has a 4m thick consolidated layer; a keel depth of 30m and a flexural strength of 350kPa. The h_k effective is 15m and the equivalent total rectangle of solid ice for bending about the z-z axis is given as

$$h = 4 + (25/350)15 = 4 + 1.1 = 5.1\text{m}$$

Continuing the example; if the ridge is 85m wide and 500m long and there is initially no penetration prior to bending failure (so that D in Eq. 7 is zero), then the load on the platform (F) when such a ridge fails by in-plane bending is

$$F = 1.33(85^2)(5.1)(350)/500\ \text{kN} = 34.3\text{MN}$$

A more modest ridge as might be seen operationally with a 2.5m thick CL layer and a 15m keel would give a load of 15MN.

It is of interest to compare these numbers to out-of-plane failure which would occur as the other potential failure mode – shown on Figure 5. This is complex failure mode involving both downward flexural failure of the consolidated layer as well as downward passive shearing of the keel rubble.

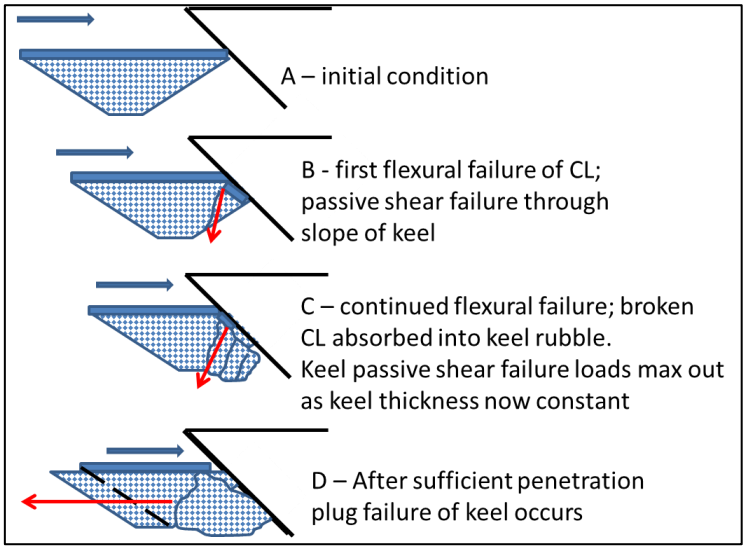

Figure 5: Downward (out-of-plane) flexural failure of a ridge

The methodology for ridge loads on sloping structures is still uncertain (no guidance in ISO 19906). One bounding approach is to use the method in ISO 19906 for keel action on a vertical structure than add the bending failure load from the consolidated layer. To apply this approach, we also need to specify the geometry of the vessel. The example chosen is one with a water line diameter of 80m, a slope angle of 45 degrees and a slope depth below the ice line of say 20m. Applying the keel method in ISO 19906 for Example 1 gives a load of 92MN. (Note this also recognizes the potential for a plug failure of the keel (see Palmer and Croasdale, 2013; Chapter 5). Applying the downward bending theory to break the consolidated layer gives 25MN for a total ridge load of 118MN. This compares to the 34MN for in-plane bending. In the second example of a 15m keel the out-of-plane load is 60MN compared to 15MN for in-plane bending.

Allowing for section loss due to penetration

The in-plane loads derived so far assume that the full cross section at the point of maximum bending is intact. This will not be the case because the interaction process will start with A and B in Figure 5. In plan view it will look like Figure 6.

The scheme to calculate the true load is shown conceptually in Figure 7.

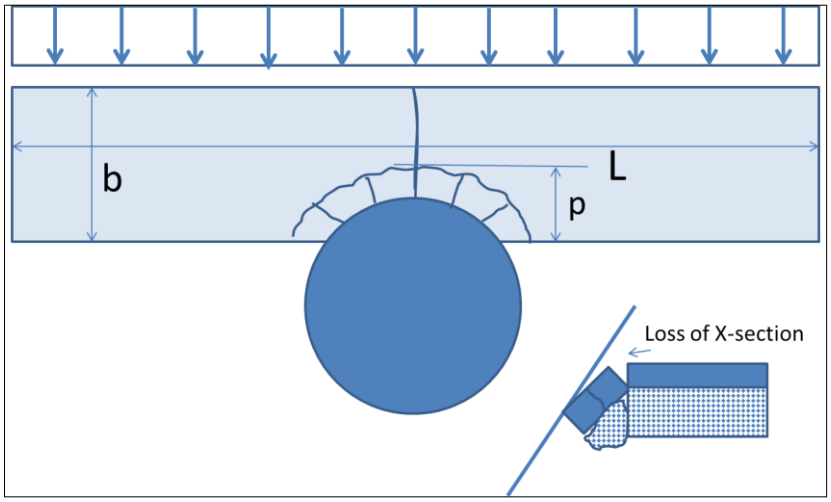

Figure 6: Initial out-of-plane ridge failure reduces the ridge cross section as the load builds up

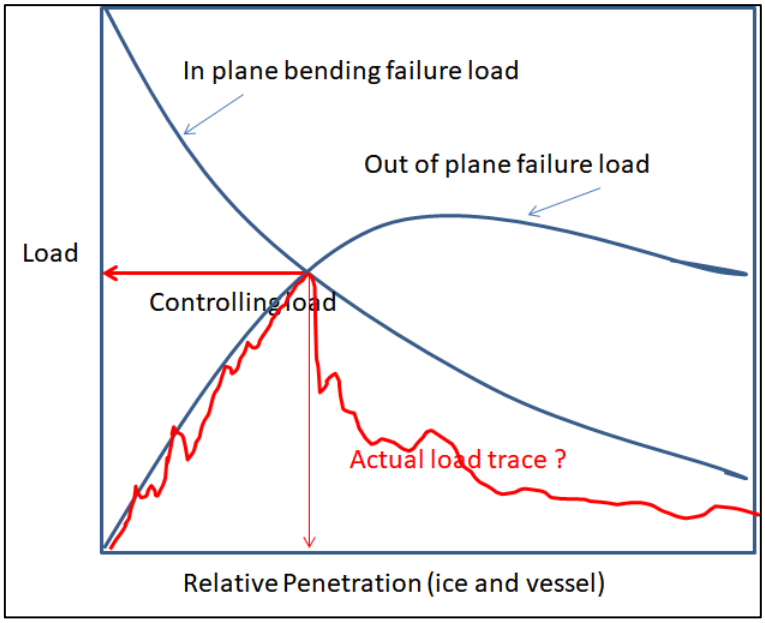

Figure 7: The scheme to find the controlling load

Load vs penetration – Example

The prior example which gave an in-plane load of 34MN is extended to include the effect of penetration on reducing the cross section. (Hence the breaking load according to the scheme shown in Figure 7).

The ultimate out-of-plane failure loads are as previously calculated, but for this calculation the load vs penetration is also needed. This is shown in Figure 8 for the keel using the previously referenced method. The controlling load is 92MN. To this is added the load to fail the consolidated layer in downwards bending.

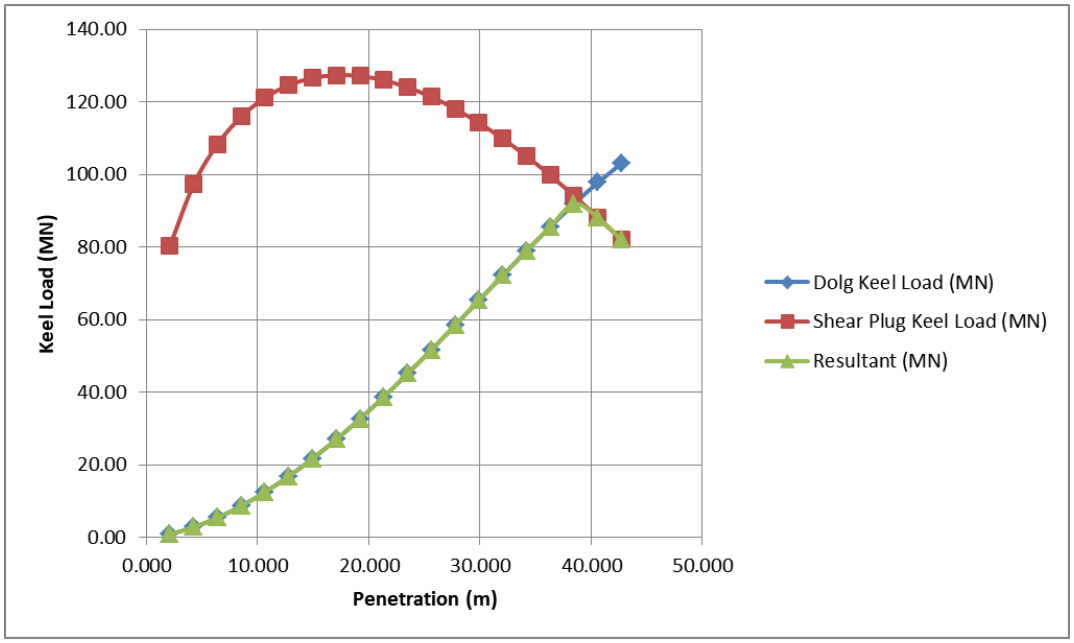

Figure 8: Load vs penetration and keel failure load

The estimated load to fail the consolidated layer (downwards) is calculated using the updated method of Croasdale et al (2016). As previously noted for Example 1, for a consolidated layer of 4m the failure load is 25MN. The build-up of this load with penetration will not be smooth but for the sake of this exercise it is assumed that the maximum value is attained at the same penetration as the maximum keel load (based on Dolgopolov). The sum of these components with penetration can now be compared to the in-plane failure load with reduced cross section as penetration proceeds. The comparison plot is shown in Figure 9:

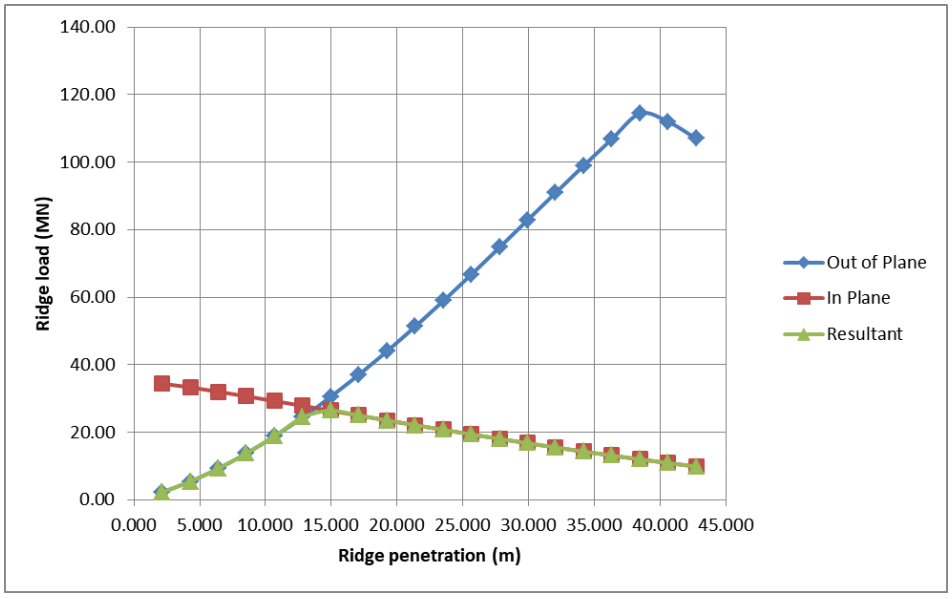

Figure 9: Ridge loads vs penetration. The controlling load is where the two curves cross

The plot in Figure 9 shows that the in-plane ridge failure load is reduced from 34MN to 26MN when loss of cross section due to penetration is accounted for.

COMPARISON WITH EXPERIMENTAL DATA

Fenz et al (2016) report on a series of model tests to investigate the process of managed ridges acting on an axi-symmetric moored floating vessel. To quote from the paper"*Three fixed factors were investigated: ridge length and ridge width to assess whether managed ridges behave as beams and whether keel depth influences managed ridge loads. The test program was conducted at HSVA in 2014 and consisted of 4 ice sheets and hence 12 ridges. With a basin width of 10m, each ridge consisted of a long fragment (5.5m), a short fragment (2.5m) and a 2m section on which ice properties were tested. There were, therefore, 24 ridge fragments available, permitting a full factorial design with three replications of each combination. Narrow ridges were 1.2m and wide ridges were 1.8m. Shallow ridges had keel depth of 25cm and deep ridges had a keel depth of 40cm. All had a consolidated layer thickness of 3.0cm. Keel rubble dimensions were 10cm x 10cm x 2.5cm for all cases. The response quantity of interest was the measured load at the time of global ridge failure."*

The model used was an axisymmetric floater with 45deg downward breaking cone at the waterline. It was moored to an underwater carriage that was advanced using the main carriage. The mooring system consisted of a four line system equivalent to a more substantial system that could be employed on an Arctic drilling vessel. The model itself consisted of two pieces: an inner structure and an outer shell connected to each other by a six component load cell. The mooring lines were attached to the inner structure, which permitted measurement of both the applied external ice load (measured by the load cell) and the static component of the response measured by the fairlead load cells. The model diameter at the water line was 1.8m.

Fenz et al (2016) did not try to compare the results with any particular theoretical models, but they provided in the paper the experimental data which allows this. Table 1 shows the experimental data and the results of calculating the in-plane ridge failure loads as described in this paper.

Table 1: Experimental data and predictions for in-plane ridge failure

															In-plane				
							0.5hk								N	N		Long	Short
Test		m	m	m	m	m	m	kPa	kPa	m	m	m	kPa	kN/m	Predicted	Measured	Prediction	only	only
		b	**penetration**	**hr**	**hcl**	**hk**	$h_{k\ effective}$	**σf**	**c**	**h**	**L**	**D**	**σ**	**w**	load	load	factor		
1010	SNL	1.20	0.48	0.220	0.029	0.191	0.10	15	0.16	0.0310	5.50	1.59	15	0.0154	84	180	**0.47**	**0.47**	
1020	SNS	1.20	0.48	0.220	0.029	0.191	0.10	15	0.16	0.0310	2.50	1.59	15	0.1451	363	238	**1.52**		**1.52**
1030	SNL	1.20	0.48	0.210	0.029	0.181	0.09	17	0.58	0.0353	5.5	1.59	17	0.0189	104	113	**0.92**	**0.92**	
1040	SNS	1.20	0.48	0.210	0.029	0.181	0.09	17	0.58	0.0351	2.5	1.59	17	0.1835	459	191	**2.40**		**2.40**
2010	DNS	1.20	0.48	0.250	0.032	0.218	0.11	18	0.15	0.0338	2.5	1.59	18	0.1878	469	235	**2.00**		**2.00**
2020	DNL	1.20	0.48	0.250	0.032	0.218	0.11	18	0.15	0.0338	5.5	1.59	18	0.0198	109	226	**0.48**	**0.48**	
2030	SWL	1.80	0.72	0.315	0.032	0.283	0.14	18	0.34	0.0374	5.5	1.76	18	0.0506	278	243	**1.15**	**1.15**	
2040	SWS	1.80	0.72	0.315	0.032	0.283	0.14	18	0.34	0.0374	2.5	1.76	18	0.5621	1405	353	**3.98**		**3.98**
2050	DWS	1.80	0.72	0.320	0.032	0.288	0.14	20	0.28	0.0360	2.5	1.76	20	0.6128	1532	283	**5.41**		**5.41**
2060	DWL	1.80	0.72	0.320	0.032	0.288	0.14	21	0.28	0.0358	5.5	1.76	21	0.0574	316	328	**0.96**	**0.96**	
3010	SNL	1.20	0.48	0.280	0.033	0.247	0.12	25	0.28	0.0357	5.5	1.59	25	0.0291	160	139	**1.15**	**1.15**	
3020	SNS	1.20	0.48	0.280	0.033	0.247	0.12	25	0.28	0.0357	2.5	1.59	25	0.2752	688	174	**3.95**		**3.95**
3030	DWL	1.80	0.72	0.355	0.033	0.322	0.16	35	0.51	0.0377	5.5	1.76	35	0.0990	544	449	**1.21**	**1.21**	
3040	DWS	1.80	0.72	0.355	0.033	0.322	0.16	38	0.51	0.0373	2.5	1.76	38	1.1907	2977	480	**6.20**		**6.20**
3050	DNS	1.20	0.48	0.265	0.033	0.232	0.12	42	0.51	0.0358	2.5	1.59	42	0.4597	1149	284	**4.05**		**4.05**
3060	DNL	1.20	0.48	0.265	0.033	0.232	0.12	42	0.51	0.0358	5.5	1.59	42	0.0486	267	226	**1.18**	**1.18**	
4010	DWS	1.80	0.72	0.365	0.032	0.333	0.17	19	0.36	0.0382	2	1.76	19	2.4202	4840	353	**13.71**		**13.71**
4020	DWL	1.80	0.72	0.365	0.032	0.333	0.17	19	0.36	0.0382	5.5	1.76	19	0.0557	306	405	**0.76**	**0.76**	
4030	SWS	1.80	0.72	0.235	0.032	0.203	0.10	17	0.39	0.0367	2.5	1.76	17	0.5171	1293	308	**4.20**		**4.20**
4040	SWL	1.80	0.72	0.235	0.032	0.203	0.10	16	0.39	0.0370	5.5	1.76	16	0.0446	245	205	**1.20**	**1.20**	
4050	DNL	1.20	0.48	0.265	0.032	0.233	0.12	20	0.20	0.0344	5.5	1.59	20	0.0216	119	159	**0.75**	**0.75**	
4060	DNS	1.20	0.48	0.265	0.032	0.233	0.12	21	0.20	0.0342	2.5	1.59	21	0.2221	555	251	**2.21**		**2.21**
										(Note: $h = hcl + h_{keffective}*(2c/\sigma f)$						Average	**2.72**	**0.93**	**4.51**
																Std Dev	**2.90**	**0.27**	**3.22**

The first point to note is that the tests were for two different lengths of ridges (L in the table), 5.5m (long) and 2.5m (short). If we look at the comparison of predicted vs measured loads, it is clear that the in-plane bending predicted load does not apply to short ridges. This is not surprising and in a personal communication it was indicated that in-plane bending failures only occurred in tests with the long ridges. Separating these tests we see that for long ridges, the average prediction factor is 0.93 (1.0 being perfect) with some scatter which is not unexpected in physical tests.

Clearly for short ridges another model needs to be used. The out-of-plane failure model has already been discussed. This was applied to the short ridges in the experimental series and the results are shown in Table 2.

Table 2: Out-of-plane ridge failures: Measured vs predicted loads

Test		hcl	hk	σf	c	L	Keel passive	Final CL bending	Predicted total	Measured	Prediction factor
		m	m	kPa	C	m	N	N	N	N	
1020	SNS	0.029	0.191	27	0.16	2.50	131	73	204	238	**0.86**
1040	SNS	0.029	0.181	33	0.58	2.5	356	77	433	191	**2.27**
2010	DNS	0.032	0.218	26	0.15	2.5	130	70	200	235	**0.85**
2040	SWS	0.032	0.283	27	0.34	2.5	338	76	414	353	**1.17**
2050	DWS	0.032	0.288	29	0.28	2.5	391	70	461	283	**1.63**
3020	SNS	0.033	0.247	33	0.28	2.5	245	84	329	174	**1.89**
3040	DWS	0.033	0.322	47	0.51	2.5	713	106	819	480	**1.71**
3050	DNS	0.033	0.232	47	0.51	2.5	389	87	476	284	**1.68**
4010	DWS	0.032	0.333	27	0.36	2	533	63	596	353	**1.69**
4030	SWS	0.032	0.203	24	0.39	2.5	283	75	358	308	**1.16**
4060	DNS	0.032	0.233	29	0.20	2.5	178	79	257	251	**1.02**
								Avg	413.36	286.36	**1.45**
								STD	172.80	82.47	**0.44**

There is a general over-prediction with the average prediction factor of 1.45. This is not surprising because the keel load method used was that in ISO 19906 for a vertical structure. In other recent work (Croasdale et al, 2018), various models for ridge loads on sloping structures have been examined and developed with comparisons made to Confederation Bridge loads. It was shown in that work that the use of the ISO 19906 keel model applied directly to a sloping structure will in general be conservative.

OTHER LIMITING MECHANISMS

Of course there are other limiting mechanisms that can apply in managed ice. An overview is given in Palmer and Croasdale, (2013) as well as in Croasdale et al, 2009. The potential loads due to short ridges calculated in this paper would unlikely be realized if some ice management of the level ice on the other side of the ridge had been accomplished. Even just releasing it from the surrounding ice could lead to the formation of a ridge building mechanism which would create a limiting driving force type situation. Creation of small floes or brash ice in the level ice would also limit to forces on the ridge fragment.

In the model tests the long ridges were 5.5m long and the short ridges 2.5m long. Taking a notional 50th scale which would make the vessel 90m in diameter, the long ridges would be 275m long and the short ridges 125m. If the surrounding ice was 1m thick and the ISO 19906 formula is used with an R value of 2000, the ridge building load would be 18.5MN compared to the out-of-plane load calculated earlier for an extreme ridge (30m keel) of 118MN and a 60MN load for ridge with a keel of 15m. If the surrounding ice was 1.5m thick the ridge building load on the 125m ridge length would be 31MN. If the ice was managed into small floes then these acting on the 125m ridge fragment should be less than about 15MN even with some ice pressure (Croasdale et al, 2009).

CONCLUSIONS

A possible optimum method of reducing loads due to first-year ridges acting on a floating system is to separate them from the surrounding level ice. This encourages them to fail by in-plane bending at lower loads compared to other failure modes. The longer the ridge the lower the resulting load so chopping up ridges into smaller lengths can actually lead to higher managed ridge loads.

A method is developed based on composite beam theory to estimate the in-plane failure loads for a range of ridge parameters. The method has been verified against experimental model test data.

It is appreciated that some ridges in nature are short, these will not fail by in-plane bending (as demonstrated in the model tests).However, separating them from the surrounding level ice can also help in encouraging ridge building upstream of the ridge at lower loads than if the ridge is frozen into the surrounding ice.

ACKNOWLEDGEMENTS

The work reported in this paper was linked to a larger project undertaken by ExxonMobil which generated the referenced model test data now in the public domain. The following individuals were part of the team; D. Fenz, R. Foltz, J. Hamilton, A. Sarlis and A. Younan. Without the initiatives taken by ExxonMobil and the named individuals, this work would not have been possible. Their contributions are gratefully acknowledged. The contents of this paper however are the sole responsibility of the author.

REFERENCES

Croasdale, K.R., Bruce, J. R., Liferov, P. (2009). Sea Ice Loads due to Managed Ice. POAC 2009, Lulea, Sweden, 2009.

Croasdale, K. R. (2012). A Simple Model for First-year Ridge Loads on Sloping Structures. ICETECH, Banff, 2012.

Croasdale K.R., Brown T.G., Li, G., Spring, W. (2018). First-year Ridge Interaction on Upward Sloping Structures: A New Approach. ATC Conference, Houston, 2018.

Dolgopolov, Y.V., Afanasiev, V. P., Koenkov, V.A., and Panilov, D. F. (1975). Effect of Hummocked Ice on the Piers of Hydraulic Structures. *Proceedings, Third IAHR Ice Symposium*, CRREL, Hanover, NH, 1975.

Fenz, D.M, Foltz, R.R., Sarlis, A. A., Younan A. H., P. Jochmann, C. Schroeder, D. Myland, G. Ziemer, and D. Spencer. (2016). Case Studies in Application of Design of Experiments Methodology to Ice Basin Testing. Arctic Technology Conference, St John's, Canada. OTC 27334.

ISO (2010) International Standards Organisation. (2010) Petroleum and natural gas industries — Arctic offshore structures. ISO 19906:2010.

Palmer, A. C. and Croasdale, K. R. "Arctic Offshore Engineering" (2013). *World Scientific Publishing Co. Ltd.*, Singapore. 2013.